Field Testing of Storm-Resilient Floating Mat Systems for Grass Cultivation and Biochar Generation

Nirmal Kumar
Prairie View A&M University
Damar David Wilson
Prairie View A&M University
Amit Singh
Old Dominion University
Bhupinder Singh
University of Houston
Abishek Kafle
University of Houston
Weihang Zhu
University of Houston
Sandeep Kumar
Old Dominion University
Ram L. Ray
raray@pvamu.edu
Prairie View A&M University
Venkatesh Balan
University of Houston

Research Article

Keywords: Floating treatment wetlands, Storm resilience, Aquatic plants, Biomass valorization, Nature-based solutions

Posted Date: June 26th, 2026

DOI: https://doi.org/10.21203/rs.3.rs-10022989/v1

Additional Declarations: No competing interests reported.

Abstract

Storm events pose significant challenges to the stability and performance of a floating treatment wetland designed to cultivate aquatic plants. This study examines the resilience and ecological performance of a floating foam mat that harbors aquatic plants, serving multiple purposes: nutrient removal (e.g., nitrate and phosphate), carbon sequestration from the atmosphere, heavy metal removal, and biochar production. Plant growth trials were conducted in a watershed using 10 modular floating mats containing two aquatic macrophytes, common rush (*Juncus effusus*) and switchgrass (*Panicum virgatum*), from mid-June to December 2025 (6 months) to assess vegetation growth, biomass composition, and pyrolysis product yields. Biomass monitoring showed that common rush had a root length of 64 cm (2'1") and a stem length of 67 cm (2'2"), while switchgrass had the highest root length of 97.5 cm (3'2") and a stem length of 128 cm (4'2") over a five-month period. The plant survival rate for each mat ranged from 90% to 92% by the end of harvesting. The CHNS analysis revealed that switchgrass roots had the highest concentrations of nitrogen (2.2%) and sulfur (0.3%). The common rush stem had higher concentrations of carbon (~ 45%) and hydrogen (~ 6%), like switchgrass. Elemental concentrations showed high potassium (K) levels (> 10,000 ppm) in both biomasses. Furthermore, pyrolyzed biomass produced the highest biochar yield at CR-PR (0.48 g/g) and SG-WR (0.42 g/g), and the lowest at CR-WC (0.35 g/g) and SG-WS (0.39 g/g). These variations in pyrolysis product amount and elemental compositions highlight differences in biomass chemical composition across plant parts. This study offers practical insights into creating storm-resilient systems that support ecological restoration and biomass valorization into pyrolysis products, such as biochar and biooil, which can be used as soil amendments and biofuels, respectively.

Introduction

Floating treatment wetlands (FTWs) remove excess nutrients, such as nitrogen and phosphorus, and heavy metals, thereby improving water quality and helping reduce algal blooms in aquatic systems, including coastal environments [1, 2]. Most research to date has focused on in situ studies of urban water [1, 3–5]. FTWs consist of buoyant foam mats planted with wetland vegetation, allowing plant roots to extend into the water column, where they support microbial biofilms that capture and filter nutrients [6, 7]. FTWs also offer key advantages over shoreline wetland establishment, including no additional land area required, adaptability to fluctuating water levels, minimal disturbance to existing habitats, and flexible placement, maintenance, and harvesting directly within the waterbody. These systems can adapt to fluctuating water levels, maintain watershed storage and flow regulation, minimize plant loss during flooding, support wildlife habitats, and be customized in both structure and plant selection [8, 9]. A floating mat system generally includes anchoring components, handling infrastructure, planting modules, and suitable aquatic plant vegetation, all designed to facilitate phytoremediation. Storm-stabilized mats further enhance resilience, supporting long-term ecological restoration [10] In this context, ecological restoration refers to the rehabilitation of aquatic ecosystem functions by stabilizing wetland vegetation on floating platforms that withstand severe rainfall and wind events [10, 11].

FTWs are constructed from a wide range of materials, including modular plastics, coconut coir, bamboo, pressure-treated wood, and waste-derived materials such as foam-to-polyvinyl chloride (PVC) pipes. Some systems also incorporate recycled polyester and polyethylene [7], typically attached to buoyant floats made of high-density polyethylene (HDPE) or fiberglass. Structural configurations vary and may be circular, rectangular, or other custom shapes [12, 13]. Previous studies have demonstrated the use of diverse FTWs designed for wastewater treatment and plant cultivation [14–18]. Design configurations play a critical role in determining plant survival and treatment efficiency. For example, one study evaluated an FTW constructed with a PVC pipe frame, plastic netting, and potholders, reporting improved water quality and enhanced ecological restoration [19]. Another investigation used low-cost, rigid plastic containers to support a two-plant system in an urban watershed receiving stormwater runoff, achieving effective oxygen transfer and coliform and nutrient removal [20]. Similarly, FTWs constructed from PVC pipes, plastic drums, and vinyl rope were tested in a eutrophic lake in Indonesia, where plants exhibited strong growth and increased biomass production [21].

In addition to the contraction material, FTW performance is influenced by environmental stressors and interactions with aquatic organisms, which affect system function, efficiency, and durability. Severe weather events, including storms, tornadoes, high temperatures, and heavy rainfall, can significantly influence aquatic plant growth [22]. Optimal pollutant removal typically occurs between 5 and 15°C, with efficiency declining outside this range [22, 23]. Rainfall and storm events can also affect plant survival, height, density, and photosynthetic surface area, potentially altering ecosystem structure [24–27]. Despite these known influences, systematic research on designing FTWs to withstand extreme climatic events or on safe mechanisms for moving them to shore for biomass harvesting remains limited.

To address the limitations of conventional FTWs under extreme weather, this study developed a storm-resilient FTW system using flexible steel-wire anchoring connected to T-posts and weighted HDPE floating mats to support the growth of common rush (*Juncus effusus*) and switchgrass (*Panicum virgatum*). Harvested biomass was converted into biochar via pyrolysis and chemical activation, enabling biomass valorization for carbon sequestration, soil improvement, and pollutant removal. Within this circular economy framework (Fig. 1), nutrient-enriched aquatic biomass is transformed into a stable, carbon-rich product that can be reused as a soil amendment, thereby closing nutrient and carbon loops, enhancing resource efficiency, and reducing waste. By integrating phytoremediation, ecosystem restoration, biomass conversion, and soil carbon management, this approach provides a climate-adaptive, scalable strategy for sustainable water treatment, wetland restoration, and the production of renewable, bio-based materials. Therefore, this study presents the design and evaluation of a storm-resilient FTW system that combines aquatic ecosystem restoration with biochar production to support the circular bioeconomy and environmental sustainability.

Materials and methods

Aquatic plant study area

The research experiment was conducted at Prairie View A&M University (PVAMU) watershed in Prairie View, Waller County, Texas, specifically in the Lower Brazos watershed (Fig. 2). This small drainage catchment/sub-watershed is associated with campus creeks, ponds, wetlands, and agricultural lands. This is one of the 6,450 Hydrologic Unit Code (HUC)-12 watersheds according to the Texas Geographic Information Office [28] The site serves as a field-scale setting for evaluating FTWs' performance under natural environmental conditions. The watershed has an irregular shape, with an approximate surface area of 2.5-3 acres and gently sloping banks lined with emergent vegetation. Specific dimensions of the watershed include area: 3.2 acres (1.28 ha, 12,763.11 m^2); perimeter: 960.8 m; and elevation ranging from 81.1 m (minimum and median) to 82.6 m (maximum). The system maintains year-round water coverage, with seasonal fluctuations driven by rainfall and evapotranspiration. Surrounding land consists primarily of open pasture with minimal tree cover along the edges, allowing natural colonization by aquatic vegetation. The site is used to evaluate phytoremediation technologies in small- to medium-scale water bodies typical of agricultural and peri-urban areas across Texas.

The PVAMU watershed was selected for its accessibility, suitable size, and nutrient-enriched conditions, providing an ideal setting to evaluate FTW performance under regionally relevant conditions. Prairie View receives ~ 1092 mm of annual rainfall, with peak precipitation in May (~ 109 mm) and the lowest in July (~ 61 mm). Rainfall occurs on roughly 134 days per year, strongly influencing the watershed's seasonal hydrology. The area also experiences severe thunderstorms; while occasional tornadoes are possible, flash flooding is common due to local soil and topography. These characteristics make the site particularly suitable for evaluating the storm resilience of floating mat systems. Collectively, these climatic and environmental features support using the PVAMU watershed as a representative field setting for testing FTWs under variable hydrological and meteorological conditions typical of comparable regional water bodies.

Applied methodology

A storm-resilient FTW system was deployed in the PVAMU watershed to evaluate its effectiveness in cultivating aquatic plants and, subsequently, producing biochar. The methodology encompassed the full process, from designing and assembling floating mats for cultivation to each step, guided by defined protocols for materials, equipment, and procedures (Fig. 3). The initial phase involved constructing a storm-resilient FTW framework of opposing T-posts connected by steel wire, anchored to concrete blocks at the bottom of the pond, to provide support and stabilization. Each structural component was secured to the floating mats with a nylon rope connected to a float for easy identification. After assembling the framework, potholes were drilled into the floating mats to accommodate one-gallon pots containing two perennial grasses (common rush and switchgrass), known for their strong root systems and high biomass production.

The plants were established in one-gallon pots placed within the floating mats. Common rush was transplanted by root division method, whereas switchgrass was established through seedling propagation, followed by plant splitting, before placement in the pots. A total of ten floating mats (M_1–M_{10}) were installed for common rush and switchgrass. The mats were arranged in two rows (R_1–R_2) to maintain spacing and enhance stability, reducing the risk of overturning during strong winds and heavy rainfall. All mats were initially planted along the shoreline to facilitate safe handling and transport. Once vegetation was established, the mats were relocated by boat to their designated positions within the watershed and secured in alignment with the T-post anchoring system.

To evaluate the performance and resilience of the floating mat systems under adverse weather, meteorological parameters, including daily rainfall from NASA GPM gauges, wind speed, evapotranspiration, potential evapotranspiration, and maximum temperature, were systematically monitored and analyzed throughout the experiment. Plant growth was documented monthly by measuring biomass accumulation and root and stem lengths. Plant conditions were closely observed, particularly before and after heavy rainfall or storm events, with development tracked through visual assessments and photographic records. Near the end of the study, plant survival rates were estimated before harvesting. Once the aquatic plants reached maturity, whole plants, including stems and roots, were harvested, and dry biomass was measured. Because both common rush and switchgrass are perennial species, only the upper stems and lower root portions were removed from each pot, allowing regrowth on the floating mats. The dried biomass was subjected to elemental analysis (CHNS) and Inductively Coupled Plasma–Optical Emission Spectroscopy (ICP-OES) to quantify metal and trace element concentrations.

A portion of the biomass was also pyrolyzed to produce biochar, which was subsequently characterized using advanced laboratory techniques. This integrated approach enabled evaluation of FTW performance in climate-adaptive biomass production and its contribution to wetland restoration.

Structure and deployment of Floating Mat Systems

The floating mat system was deployed by placing mats on the watershed surface and inserting aquatic plants into pre-cut planting holes. A high-density polyethylene (HDPE) mat with superior buoyancy and UV resistance (Magshion, USA) was used, supported by a robust anchoring system [29] HDPE was selected for its low specific gravity (0.95), UV durability, and structural strength. Each mat measured 1.83 m × 2.13 m × 0.013 m (6' × 7' × 0.5"), providing optimal spacing for plant growth. Sixty-five evenly spaced holes, 0.17 m (6.5") in diameter and sized for 1-gallon nursery pots, were cut with 0.31–0.36 m (12–14") spacing to prevent root entanglement and ensure uniform growth. The symmetrical layout also distributes weight evenly and maximizes surface utilization. Perimeter stabilization was achieved using ~ 9 mm (3/8") marine-grade nylon ropes threaded through reinforced edge eyelets. A hybrid anchoring system consisting of steel wires tensioned between T-posts, 25 lbs concrete blocks at the watershed base, and nylon rope connections secured the floating mats while allowing limited vertical movement during water-level fluctuations and preventing lateral drift under severe weather conditions (Fig. 3).

The 65 precision-cut planting holes enable flexible, scalable plant arrangements, while the mat design supports three critical functions: (1) maintaining structural tension to keep the mat flat, (2) enabling secure connection to anchoring systems, and (3) allowing modular interconnection for multiple mats. Rope channels were thermoformed during HDPE fabrication

to reduce abrasion, and stainless-steel grommets were installed at stress points to enhance durability. Perimeter ropes were connected to concrete blocks using galvanized carabiners, forming a secure yet adjustable mooring system that accommodates changing water levels.

Criteria for plant selection and recommended planting methods

Common rush (*Juncus effusus*) and switchgrass (*Panicum virgatum*) were selected for their adaptability to wetland and southern Texas conditions, high nutrient uptake, and robust root systems that support nutrient filtration and microbial activity [30, 31]. Switchgrass, a native warm-season grass, develops an extensive root system and produces high biomass, making it effective for nutrient removal and offering considerable bioenergy potential [31, 32]. Together, these species provide complementary functions that enhance water quality and support FTW-based remediation. These native plants are well-adapted to local conditions and require minimal maintenance. Two planting methods were used: rooted transplants of common rush collected from PVAMU and switchgrass seedlings.

Assessment of severe weather impacts

Meteorological observations were recorded to assess the resilience of floating mat systems under severe weather conditions. Daily rainfall data were obtained from the NASA GPM gauge[33] (PIERS-0034-GPM 034) near the PVAMU watershed. Floating mat performance was analyzed under two rainfall categories: light-to-moderate rainfall (< 30 mm) and moderate-to-heavy rainfall (30–70 mm/day). Additional weather parameters, including maximum temperature[34], potential evapotranspiration (PET) [35], and wind speed, were also considered to assess the mats' performance under varying and extreme environmental conditions (Table S1).

Plant-grown monitoring

The next phase of the methodology focused on monitoring plant growth, assessing biomass accumulation (stem and root lengths), and estimating plant survival rates prior to harvesting. Biomass accumulation was recorded monthly using representative plants from each floating mat [7, 36, 37]. Plant survival rate was calculated using the following equation:

$$Plant\ survival\ rate = \frac{Healthy\ Plants}{Total\ Planted}\text{x}100 \quad (1)$$

In this study, the target was 65 plants per mat, and only those surviving at harvest were considered healthy. Once the plants matured, they were harvested, and dry biomass was measured. Consistent with their perennial nature, only the upper stems and lower roots were removed, leaving the remaining portion on the mats to allow regrowth. The harvested dry biomass, including both roots and stems, was transported for biochar production.

Biomass pyrolysis

Common rush and switchgrass were collected from different zones within the floating system (watershed, edge, and pool), although switchgrass was obtained only from the watershed. Samples designated for biochar production were air-dried and stored in a dry room prior to processing. Pyrolysis was conducted in a 500 ml Parr batch reactor under a nitrogen atmosphere; the reactor was purged with N_2 at 10 psi for 5 minutes before heating. Biomass (5–8 cm particle size, 15–30 g loading) was heated at 9.7°C/min to 450°C and held for 30 min to produce biochar, while bio-oil and gases were not quantified.

After cooling, biochar was recovered and weighed directly. Moisture and ash contents of biomass and biochar were determined according to NREL Laboratory Analytical Procedures [38–39], and the dry-basis biochar yield was calculated using Eq. (2). The reactor configuration has been described in previous studies [38, 39]. The biochar yield on a dry basis was measured using Eq. (2).

$$\text{Yield} = \frac{\text{Amount of biochar (g)}}{\text{Amount of biomass (g)}} \tag{2}$$

The reactor configuration has been described in previous studies [40–42]

CHNS and ICP-OES analysis

Two grasses were harvested from FTWs and separated into above- and below-ground biomass, washed to remove sediment, and oven-dried at 65°C to constant weight. The dried plant samples were finely ground using a ball mill and analyzed for elemental composition (C, H, N, S) using a FlashSmart CHNS Elemental Analyzer (Thermo Fisher Scientific), which employs dynamic flash combustion followed by gas chromatography for high-precision quantification[43]. Calibration was performed with certified standards, including acetanilide and sulfanilamide. For metal analysis, 250 mg of the finely ground plant powder was accurately weighed into clean digestion tubes and documented. Each tube received 7 mL of concentrated HNO_3, and the samples were placed in a digestion system. The temperature was gradually increased from 80°C to 120°C and maintained at 120°C for 1 hour and 15 minutes. Subsequently, 2 mL of 30% H_2O_2 was added, and the tubes were allowed to cool to room temperature. The digested solutions were transferred into 25 mL volumetric flasks, rinsing the tubes with deionized (DI) water, and the volume was adjusted to 25 mL with DI water. The solutions were filtered through 0.45 μm membrane filters to remove particulates, and the clear filtrates were collected in acid-washed polyethylene vials for subsequent analysis using Inductively Coupled Plasma–Optical Emission Spectroscopy (ICP-OES).

Results and discussion

Biomass growth monitoring

We conducted monthly monitoring of aquatic plant biomass (Fig. S1). During severe weather events, biomass health was also assessed through physical inspection and photographic documentation. The PVAMU watershed frequently experiences intense storms, particularly in the summer months of June to August, driven primarily by hurricanes originating over the Atlantic Ocean and the Gulf of Mexico. Accordingly, the floating mat system's storm resilience was evaluated under these conditions. Biomass health was assessed starting on the day of planting common rush and switchgrass in June 2025. Monitoring began in June 2025, at the time of planting common rush and switchgrass. Common rush roots grew around 6 cm (2.3") across the mats within 1.5 months, confirming successful establishment via transplanted roots (Fig. S1a). Switchgrass, planted using a split-plot method to reduce planting costs, showed more vigorous early growth. Its roots reached 18 cm (7.1") shortly after planting (Fig. S1b).

By October 2025, biomass levels had increased substantially across all mats. Measurements were recorded for all 10 floating mats arranged in two rows. For mat M1R1, the maximum root length was 48.8 cm (1'6"), and the stem length was 67.1 cm (2'2") (Fig. 4a–b). Among the eight common rush mats, M_1R_1 and M_8R_2 exhibited the highest growth, with root lengths of 64 cm (2'1") and stem lengths of 67 cm (2'2"). In contrast, switchgrass showed superior growth, with maximum root and stem lengths of 97.5 cm (3'2") and 128 cm (4'2"), respectively (Fig. 4c–d), underscoring its greater biomass potential relative to common rush.

Previous studies have shown that switchgrass exhibits greater root growth than other species, such as bush clover (*Lespedeza davurica S.*), under varying water and treatment conditions [44]. Switchgrass can also develop extensive root systems, reaching depths of 5–6 feet [45] In our experiment, final root and stem lengths were measured for both species on each floating mat. Average root and stem lengths increased over time, with switchgrass showing the most significant growth, followed by common rush (Fig. 5). Growth continued through October but slowed thereafter, likely due to reduced sunlight during the winter months. Similarly, other studies have reported peak switchgrass biomass yields in October [46]. Overall, analysis of root and stem lengths over time showed that switchgrass exhibited the greatest growth, followed by common rush, throughout the harvesting period.

Harvesting of mature aquatic plants

Two grasses were harvested during the second week of December 2025, marking a cultivation period of ~ 5–6 months from potting to harvest. As perennials, both species were partially retained after harvest: the upper stems were cut, leaving 5–8 cm above the one-gallon pot neck, and the lower roots were trimmed, leaving 5–8 cm at the pot base (Fig. S2), allowing the plants to regrow in the same floating mat holes. Dry biomass measurements showed that switchgrass produced the highest total biomass, followed by common rush (Fig. 5c), followed by the lowest biomass of 750 g. In the case of common rush, 422 g was the highest biomass of a single plant, and 121 g was the lowest biomass of a single plant. These findings align with previous reports of high biomass production in switchgrass [46, 47]

Overall, these results demonstrate that floating mats can support the cultivation of aquatic plants and achieve substantial biomass yields within five to six months, even under gusty winds and heavy rainfall. Given the study's primary goal of linking biomass production to biochar generation, the performance of storm-resilient FTWs was further evaluated for their potential in biomass valorization through pyrolysis.

CHNS analysis

CHNS analysis of common rush samples collected from three locations (watershed, edge, and swimming pool) and of switchgrass from the watershed revealed variability in elemental composition, reflecting differences in environmental conditions during growth (Fig. 6). Higher carbon (%) generally corresponds to greater organic matter concentration [48, 49] Among common rush samples, the common rush-watershed stem (CR-WS), common rush-pool stem (CR-PS), and common rush-edge stem (CR-ES) exhibited elevated carbon levels, reflecting substantial organic matter content. In contrast, the common rush-watershed root (CR-WR), common rush-pool root (CR-PR), and common rush-edge root (CR-ER) had lower carbon and hydrogen concentrations, with CR-WR showing the lowest values. Additionally, CR-WS, CR-PS, and CR-ES contained higher hydrogen content than the root samples. Similarly, the switchgrass-watershed stem (SG-WS) exhibited higher carbon and hydrogen levels compared to the switchgrass-watershed root (SG-WR).

For nitrogen, SG-WR exhibited the highest concentrations, followed by CR-ER, while SG- WS had the lowest. The elevated nitrogen content in SG-WR indicates enhanced nutrient uptake and allocation by grass roots, consistent with field observations that increased nitrogen availability raises root N concentrations and lowers C: N ratios [50]. In our case, C: N ratios were lowest for SG-WR, followed by CR-WR, with minimal standard deviation, indicating strong consistency across replicates. Sulfur (S%) remained the lowest element across all samples, though SG-WR and CR-ER showed the highest S concentrations.

Overall, CHNS analysis revealed clear differences between common rush and switchgrass across locations, with carbon (%) predominating in all samples and the highest values typically observed in stems. C: N and C: H ratios were also calculated to evaluate the potential for carbon storage and nutrient retention in FTW-cultivated aquatic plants. SG-WS and common rush-pool stem (CR-PS) exhibited the highest C: N ratios, whereas SG-WR showed the lowest C: H ratios, mirroring its C: N pattern. Common rush-pool root (CR-PR) and CR-ER exhibited higher C: H ratios. These results highlight distinct elemental and nutritional fingerprints associated with species type and environmental conditions.

ICP-OES analysis

ICP-OES analysis revealed the elemental composition of the aquatic plant samples, including major elements potassium (K), magnesium (Mg), and sodium (Na), as well as trace metals such as manganese (Mn) and zinc (Zn), and the essential nutrient phosphorus (P) (Fig. 7) [51]. Potassium was the most abundant element in most samples, with the highest concentrations in CR-WS and switchgrass, indicating substantial potassium enrichment. This aligns with findings from a previous study.

Switchgrass biomass is typically dominated by K, followed by P, Mg, Na, and Zn [52] Magnesium and Manganese showed considerable variability across samples, largely influenced by species and site-specific conditions, with switchgrass generally exhibiting higher concentrations [53] Furthermore, SG-WR showed elevated levels of phosphorus and zinc compared with other samples. Sodium concentrations were higher in edge-common rush and pool-specific samples than in the other plants. While phosphorus levels were generally lower, they were notably higher in switchgrass and certain edge samples, underscoring their role in nutrient accumulation. Zinc was present in all samples at relatively low concentrations, with slightly higher levels in edge and watershed samples. Overall, elemental enrichment was more pronounced in switchgrass across most elements, except for sodium, which tended to be higher in common rush from edge and pool locations. These results highlight species-specific nutrient accumulation patterns and the influence of local environmental conditions on the elemental composition of aquatic plants cultivated in floating treatment wetlands.

Storm impact analysis

Heavy rainfall accompanied by gusty winds can affect FTW systems, potentially causing mat dislocation, anchoring stress, and plant uprooting [54]. To evaluate their resilience, we monitored floating mats during severe weather conditions from mid-June to December 2025 (6 months). Moderate to heavy rainfall was recorded across the watershed, with June and September experiencing the highest precipitation, exceeding 50 mm (Fig. S3). In our study, two intense rainfall events occurred in June and August 2025, each exceeding 50 mm, while the remaining events were below 30 mm. Severe rainfall, particularly during hurricanes, is known to be highly destructive to vegetation [55] For example, Hurricane Harvey in 2018 caused widespread vegetation damage in the region surrounding its confluence[26].Given that the PVAMU watershed is in a hurricane-prone area, FTW systems are potentially vulnerable to such extreme weather events. Despite this, continuous monitoring of the cumulative six-month rainfall, combined with visual inspections and biomass measurements, showed no significant impact on the floating plants. The mats remained securely anchored, and the plants continued to grow healthily and consistently throughout the study period. In this region, gusty winds typically accompany heavy rainfall. Wind speeds of 3–8 m/s are considered normal breezes and generally do not harm plant stems, whereas speeds exceeding 8 m/s can damage the stems of aquatic plants.

Although Real-Time Mesoscale Analysis (RTMA) datasets indicated that wind speeds did not exceed 6 m/s, we observed that common rush and switchgrass on the floating mats were aligned in a single direction during heavy rainfall (Fig. S4a). This may reflect gusty winds associated with rainfall that were not captured by the coarse-resolution (2.5 km) RTMA data. According to RTMA records, daily wind speeds ranged from 1.5 to 6 m/s, which is considered mild and generally insufficient to damage plants. The absence of in situ wind-speed measurements suggests that RTMA data may underestimate short-duration gusts.

Despite this, floating mats were displaced from their original positions during heavy rainfall (Fig. S4b), and some common rush plants on a few mats were disturbed or damaged. These observations indicate that heavy rain, sudden gusts, and wave action can stress floating platforms and crops even when sustained wind speeds are moderate. Other weather parameters, including maximum temperature and PET, were also monitored to assess plant growth. Maximum temperatures across the watershed ranged from 8 to 37°C, while PET ranged from 1.5 to 6.28 mm (Fig. S5). Temperatures remained consistently high (> 32°C) from June to October, then declined with the onset of early winter. PET was moderate to high through October, then decreased to its minimum. Warm temperatures and moderate PET during summer and early autumn likely promoted the growth and biomass production of common rush and switchgrass on the mats. By the December harvest, lower temperatures and PET prevailed, yet no plant or mat damage was observed. Overall, the floating mat system and its plants demonstrated resilience across all weather conditions during the 2025 monitoring period.

Structural integrity, system stability, and plant survival rate

The structural integrity of the floating mats was carefully monitored to assess their resilience throughout the study period. During storm events, individual mats were occasionally displaced from their original positions, often accumulating near the watershed edge (Fig. S4b). Although each mat was anchored with a 25 lbs concrete block to provide downward stability, some were moved by strong winds or wave action. In several instances, dislocation was also attributed to damage to the nylon ropes connecting the mats to the underwater concrete anchors; turtles were occasionally observed biting the ropes, which allowed the mats to become partially free. Additionally, a few plants, along with their pots, were lifted from the pre-cut holes in the mats by rising water currents or strong winds. Despite these disturbances, the row-wise arrangement of mats at equal spacing prevented overall deformation, tilting, or overlapping, preserving the structural layout of the FTW system. Increasing the weight of the concrete anchors could further improve stability during extreme weather events. Plant survival was assessed for each mat in both rows. For common rush, nearly all mats retained 59–62 plants out of the 65 initially planted, corresponding to a survival rate of approximately 90–95%. Switchgrass showed comparable survival, indicating that both species remained resilient under field conditions, even during heavy rainfall and gusty winds. These results indicate that the floating mats, combined with strategic anchoring and row-wise spacing, effectively supported plant stability and persistence under challenging environmental conditions.

Biomass valorization using pyrolysis

Biochar was produced via controlled pyrolysis of common rush and switchgrass biomass, yielding 0.35–0.48 g/g depending on feedstock type (Fig. 8), consistent with reported values for lignocellulosic materials under slow pyrolysis conditions [56] Pyrolysis involves the sequential thermal degradation of biomass components: initial drying (up to ~ 150°C) removes free and bound moisture with minor volatile loss (2–8%), followed by active pyrolysis (150–600°C), during which major mass loss (60–70%) occurs as hemicellulose, cellulose, and part of lignin decompose.

Hemicellulose degrades first (100–300°C) due to its low thermal stability, followed by cellulose breakdown (300–600°C), producing CO, CO_2, and other volatiles through depolymerization and fragmentation pathways [57] Lignin decomposes more gradually over a broad temperature range (100–900°C), contributing significantly to char formation due to its aromatic structure and high thermal stability [58] In the final stage (above ~ 600°C), residual lignin undergoes slow degradation, further enhancing biochar yield, while hemicellulose and cellulose generate gases and oxygenated compounds, including CH_4, CO_2, CO, H_2, carboxylic acids, aldehydes, and other light organics [59]

The Waterloo mechanism, widely used to describe cellulose pyrolysis, involves three primary pathways: (i) fragmentation, producing low-molecular-weight oxygenates such as acids, alcohols, and carbonyl compounds; (ii) depolymerization, yielding anhydrosugars, including levoglucosan; and (iii) dehydration, producing char, water, and permanent gases [14] Biochar formation is further enhanced during lignin decomposition, which also generates condensable vapors, liquid aerosols, and non-condensable gases [60] In general, higher biochar yields reflect greater retention of solid carbon and ash, whereas lower yields indicate greater conversion to vapors and gases. Biochar properties are strongly influenced by feedstock composition and process parameters, including temperature, residence time, heating rate, and particle size [61] Thus, yield variations across samples, even under identical operating conditions, reflect differences in biomass characteristics, collection location, and reactor behavior [62]

These differences are primarily due to variation in biomass composition, as indicated by CHNS analysis (Fig. 6). Even within the same FTW system, cellulose, hemicellulose, lignin, and ash contents can vary among samples. Lignin contributes more to char formation because of its aromatic, thermally stable structure, whereas cellulose and hemicellulose preferentially form volatile products. Inorganic minerals also remain in the solid residue, increasing the apparent biochar yield. Accordingly, samples with higher lignin or ash content are expected to produce greater yields, whereas those richer in volatile-forming fractions yield less biochar. This compositional effect aligns with the higher yields observed in CR-ES (0.47 g/g), CR-PR (0.48 g/g), and CR-PC (0.44 g/g) compared with CR-WC (0.35 g/g) and CR-WS (0.38 g/g) [63]

Biomass collection location likely influences biochar yield by affecting plant growth, nutrient uptake, and tissue development, as well as moisture and mineral content, all of which affect pyrolysis behavior. Wetland-associated plants are particularly sensitive to local environmental conditions, and differences in water and soil regimes can alter the mineral accumulation retained in biochar after pyrolysis. In addition, spatial variation in growth stage and plant structure may affect biochemical composition, including lignin content. Therefore, the observed differences in common rush biochar yield are likely driven by location-dependent variations in chemical and mineral composition, whereas switchgrass shows less variability because it is collected from a single watershed environment [64, 65]

Accurate interpretation of yield also depends on the calculation basis. In this study, dry-basis biochar yield was determined using Eq. (2), which accounts for moisture in both biomass and biochar. The average moisture content was 7.4 wt.% for biomass and 1.9 wt.% for biochar, ranging from 6.3 wt.% (CR-ES) to 7.9 wt.% (CR-PR). Ash content in biomass averaged 7.2 wt.% and varied widely from 2.1 wt.% (CR-ES) to 15.5 wt.% (CR-PR), indicating substantial heterogeneity in inorganic matter that likely contributed to differences in pyrolysis behavior and biochar yield.

Overall, the results indicate that biochar yield is governed by biomass composition, collection location within the floating system, pyrolysis conditions, and calculation basis. Samples with higher lignin and ash contents, incomplete devolatilization, or enhanced vapor–solid interactions tended to yield more char, whereas those richer in volatile fractions or subjected to more effective heat transfer yielded less char. Thus, the observed behavior reflects both intrinsic biomass pyrolysis characteristics and reactor-specific thermal and transport effects, providing a more rigorous framework for interpreting the potential of common rush and switchgrass as biochar feedstocks [66–68].

Pyrolysis yields and elemental compositions are shown in Figs. 6 and 8. CHNS analysis of CR-WC was used to track carbon transformation from biomass to biochar, and the Van Krevelen approach was used to assess coalification during thermal conversion. The H/C ratio decreased from 1.34 in CR-WC biomass to 0.42 in the corresponding biochar, indicating significant carbonization through loss of hydrogen-rich volatiles and formation of a more condensed aromatic structure, consistent with enhanced structural stability and coalification. These results further highlight the influence of species, plant fraction, and growth location on biomass chemistry and pyrolysis behavior, underscoring the importance of optimizing feedstock selection to improve biochar production and valorization in FTW systems.

Limitations and challenges of the study

The present findings underscore the need for further design improvements to enhance the stability and operational feasibility of floating mat systems. Mat displacement observed under high-wind conditions aligns with previous FTW studies, which identified anchoring limitations and deformation of interconnected mats as major constraints on long-term performance [69] Stability could be improved by using heavier anchoring weights (e.g., ~ 40 lb concrete blocks) to better resist storm-induced forces. In addition, interactions with local fauna, such as turtles biting nylon ropes and occasional observations of snakes resting on mats, highlight the influence of wildlife on system integrity and mobility during storm events. While HDPE mats offer durability for plant cultivation, prolonged exposure to intense solar radiation may lead to material degradation and the potential release of microplastics, raising sustainability concerns.

These limitations underscore the need to explore low-cost, non-plastic, or hybrid-floating alternatives for long-term sustainability. Promising options include natural fiber–based mats (e.g., coconut coir, jute, bamboo, or reed bundles), bio-composite rafts, and biodegradable polymer–reinforced frames, which can reduce plastic use while maintaining buoyancy and plant support. Such systems may be particularly advantageous for large-scale or resource-limited applications where environmental compatibility is a priority. Floating mat systems are generally better suited to subtropical and temperate climates, where materials are more durable; however, in tropical conditions, more robust or replaceable designs may be required due to greater environmental stress. Finally, plant loading is constrained by buoyancy capacity; for the present mat dimensions (1.83 m × 2.13 m × 0.013 m), each unit supports approximately 65–70 one-gallon plants while maintaining structural stability and adequate flotation.

Conclusion

This study presents an advanced floating treatment wetland (FTW) system designed as a scalable approach for aquatic plant restoration under extreme weather conditions while enabling biomass valorization. The system employs HDPE floating mats, concrete anchors, and opposing T-posts connected by steel cables to enhance storm resilience. Over six months (July–December 2025), common rush and switchgrass were cultivated in one-gallon pots to evaluate system performance, showing strong growth and a 90–92% survival rate despite multiple heavy rainfall and wind events. Switchgrass produced the highest biomass (1.1 kg), followed by common rush (421 g). The installation comprised 10 floating mats (6 × 7 ft each), covering ~ 0.31% of a 12,763 m² pond and supporting ~ 650 1-gallon plant pots, yielding ~ 186 kg of biomass and an estimated ~ 89 kg of biochar after pyrolysis. Higher biochar yields were observed from root biomass, confirming its suitability as a superior feedstock for carbon-rich char production. CHNS-based estimates further indicated that the harvested biomass corresponded to the removal of ~ 2.0 kg nitrogen and ~ 0.15 kg phosphorus, along with ~ 78 kg carbon sequestration (~ 286 kg CO_2 equivalent), demonstrating strong nutrient uptake and climate mitigation potential. Collectively, the system integrates storm-resilient FTW design with biochar production to simultaneously support water quality improvement, nutrient recovery, and carbon sequestration. Future improvements should focus on enhancing anchoring stability and adopting more durable, low- or non-plastic materials to extend system lifespan and broaden applicability across diverse environmental conditions.

Abbreviations

CR-ER
Common rush-edge root
CR-ES
Common rush-edge stem
CR-EC:
Common rush-edge combined
HPDE
High-Density Polyethylene
K
Potassium
Mg
Magnesium

Mn
Manganese
Na
Sodium
CR-PS:
Common rush-pool stem
CR-PR
Common rush-pool root
CR-SPC
Common rush-pool combined
P
Phosphorus
CR-WR
Common rush-watershed root
CR-WS
Common rush-watershed stem
CR-WC
Common rush-watershed combined
SG-WR
Switchgrass-watershed root
SG-WS
Switchgrass-watershed-stem
SG-WC
Switchgrass-watershed-combined
Zn
Zinc

Declarations

The authors declare no competing interests

Author Contribution

Conceptualization N.K., V.B., R.L.R.; methodology, N.K., V.B., R.L.R., D.D.W., A.S., and S.K.; investigation, N.K., V.B., R.L.R., D.D.W., A.S., and S.K.; writing original draft preparation, N.K., V.B., R.L.R., A.S., D.D.W., B.S., A.K.; writing review and editing, N.K., V.B., R.L.R., A.S., S.K., B.S., A.K.; visualization, V.B., R.L.R.; supervision, V.B. and R.L.R.; funding acquisition, V.B., R.L.R., S.K., and W.Z. All authors have read and agreed to the published version of the manuscript.

Acknowledgement

This manuscript was made possible by funding from the Environmental Protection Agency (EPA#02D48123). Some of the funds from the United States Department of Agriculture (USDA#xxxxxx) were used to produce biochar. We also thank the UH Center for Carbon Management and Energy (CCME) for supporting V.B. with a small research grant. We thank Beemats LLC, in Florida, for donating the floating mat used in the project's initial phase.

Data availability

The datasets generated or analyzed during the current study will be available upon request.

References

1. Sharma R, Vymazal J, Malaviya P (2021) Application of floating treatment wetlands for stormwater runoff: A critical review of the recent developments with emphasis on heavy metals and nutrient removal. Science of the Total Environment 777
2. Maxwell B, Winter D, Birgand F (2020) Floating treatment wetland retrofit in a stormwater wet pond provides limited water quality improvements. Ecol Eng 149:. https://doi.org/10.1016/j.ecoleng.2020.105784
3. Colares GS, Dell'Osbel N, Wiesel PG, et al (2020) Floating treatment wetlands: A review and bibliometric analysis. Science of the Total Environment 714
4. Nichols P, Lucke T, Drapper D, Walker C (2016) Performance evaluation of a floating treatment wetland in an urban catchment. Water (Switzerland) 8:. https://doi.org/10.3390/W8060244
5. Yeh N, Yeh P, Chang YH (2015) Artificial floating islands for environmental improvement. Renewable and Sustainable Energy Reviews 47:616–622
6. Rehman K, Ijaz A, Arslan M, Afzal M (2019) Floating treatment wetlands as biological buoyant filters for wastewater reclamation. Int. J. Phytoremediation 21:1273–1289
7. Kumar N, Singh B, Chen Y, et al (2025) The Bioremediation of Nutrients and Heavy Metals in Watersheds: The Role of Floating Treatment Wetlands. Applied Sciences (Switzerland) 15
8. Colares GS, Dell'Osbel N, Wiesel PG, et al (2020) Floating treatment wetlands: A review and bibliometric analysis. Science of the Total Environment 714
9. S.C. Calheiros C, Ilarri M, Godinho M, et al (2025) Biodiversity assessment in a floating treatment wetland established in a stormwater pond. Ecol Eng 215:. https://doi.org/10.1016/j.ecoleng.2025.107598
10. Rome M, Happel A, Dahlenburg C, et al (2023) Application of floating wetlands for the improvement of degraded urban waters: Findings from three multi-year pilot-scale installations. Science of the Total Environment 877:. https://doi.org/10.1016/j.scitotenv.2023.162669

11. Xu B, Wang X, Liu J, et al (2017) Improving Urban Stormwater Runoff Quality by Nutrient Removal through Floating Treatment Wetlands and Vegetation Harvest. Sci Rep 7:. https://doi.org/10.1038/s41598-017-07439-7
12. Hartshorn N, Marimon Z, Xuan Z, et al (2016) Complex interactions among nutrients, chlorophyll-a, and microcystins in three stormwater wet detention basins with floating treatment wetlands. Chemosphere 144:408–419. https://doi.org/10.1016/j.chemosphere.2015.08.023
13. Winston RJ, Hunt WF, Kennedy SG, et al (2013) Evaluation of floating treatment wetlands as retrofits to existing stormwater retention ponds. Ecol Eng 54:254–265. https://doi.org/10.1016/j.ecoleng.2013.01.023
14. Shen S, Li X, Lu X Recent developments and applications of floating treatment wetlands for treating different source waters: a review. https://doi.org/10.1007/s11356-021-16663-8/Published
15. Wei F, Shahid MJ, Alnusairi GSH, et al (2020) Implementation of floating treatment wetlands for textile wastewater management: A review. Sustainability (Switzerland) 12:1–29. https://doi.org/10.3390/su12145801
16. Wang CY, Sample DJ (2014) Assessment of the nutrient removal effectiveness of floating treatment wetlands applied to urban retention ponds. J Environ Manage 137:23–35. https://doi.org/10.1016/j.jenvman.2014.02.008
17. Weragoda SK, Jinadasa KBSN, Zhang DQ, et al (2012) Tropical application of floating treatment wetlands. Wetlands 32:955–961. https://doi.org/10.1007/s13157-012-0333-5
18. Colares GS, Dell'Osbel N, Wiesel PG, et al (2020) Floating treatment wetlands: A review and bibliometric analysis. Science of the Total Environment 714
19. Nuruzzaman M, Anwar AHMF, Sarukkalige R (2023) Computational fluid dynamics modeling of floating treatment wetland retrofitted stormwater pond: Investigation on design configurations. J Environ Manage 337:. https://doi.org/10.1016/j.jenvman.2023.117746
20. Olguín EJ, Sánchez-Galván G, Melo FJ, et al (2017) Long-term assessment at field scale of Floating Treatment Wetlands for improvement of water quality and provision of ecosystem services in a eutrophic urban pond. Science of the Total Environment 584–585:561–571. https://doi.org/10.1016/j.scitotenv.2017.01.072
21. Henny C, Jasalesmana T, Kurniawan R, et al (2020) The effectiveness of integrated floating treatment wetlands (FTWs) and lake fountain aeration systems (LFAS) in improving the landscape ecology and water quality of a eutrophic lake in Indonesia. In: IOP Conference Series: Earth and Environmental Science. Institute of Physics Publishing
22. Van De Moortel AMK, Meers E, De Pauw N, Tack FMG (2010) Effects of vegetation, season and temperature on the removal of pollutants in experimental floating treatment wetlands. Water Air Soil Pollut 212:281–297. https://doi.org/10.1007/s11270-010-0342-z
23. Varma M, Gupta AK, Ghosal PS, Majumder A (2021) A review on performance of constructed wetlands in tropical and cold climate: Insights of mechanism, role of influencing factors, and system modification in low temperature. Science of the Total Environment 755

24. Zhang Y, Li T, Zhang L, et al (2024) Effects of extreme rainfall events on phytoplankton community in a subtropical eutrophic lake: a mesocosm experiment. Israeli Journal of Aquaculture - Bamidgeh 76:. https://doi.org/10.46989/001c.92652
25. Correia KM, Smee DL (2022) A Meta-analysis of Tropical Cyclone Effects on Seagrass Meadows. Wetlands 42:. https://doi.org/10.1007/s13157-022-01611-0
26. Stagg CL, Osland MJ, Moon JA, et al (2021) Extreme precipitation and flooding contribute to sudden vegetation dieback in a coastal salt marsh. Plants 10:. https://doi.org/10.3390/plants10091841
27. Lin TC, Hogan JA, Chang C Te (2020) Tropical Cyclone Ecology: A Scale-Link Perspective. Trends Ecol. Evol. 35:594–604
28. Texas Geographic Information Office (TxGIO) StratMap Hydrography Program
29. Lange K, Jönsson E, Österlund H, et al (2024) Floating Treatment Wetlands Made of HDPE and PET Can Be Sources of Microplastics. J Sustain Water Built Environ 10:. https://doi.org/10.1061/jswbay.sweng-576
30. Rodriguez-Dominguez MA, Biller P, Carvalho PN, et al (2021) Potential use of plant biomass from treatment wetland systems for producing biofuels through a biocrude green-biorefining platform. Energies (Basel) 14:. https://doi.org/10.3390/en14238157
31. Aaron Hockensmith J, State M (2024) Evaluating the emergent wetland plant Juncus effusus as a tool in phytoremediation of nitrogen and copper
32. Yang J, Worley E, Ma Q, et al (2016) Nitrogen remobilization and conservation, and underlying senescence-associated gene expression in the perennial switchgrass Panicum virgatum. New Phytologist 211:75–89. https://doi.org/10.1111/nph.13898
33. Petersen WA, Kirstetter P-E, Wang J, et al (2020) The GPM Ground Validation Program. pp 471–502
34. De Pondeca MSF V., Manikin GS, DiMego G, et al (2011) The Real-Time Mesoscale Analysis at NOAA's National Centers for Environmental Prediction: Current Status and Development. Weather Forecast 26:593–612. https://doi.org/10.1175/WAF-D-10-05037.1
35. Abatzoglou JT (2013) Development of gridded surface meteorological data for ecological applications and modelling. International Journal of Climatology 33:121–131. https://doi.org/10.1002/joc.3413
36. (2018) Part 158 Nontarget Plant Protection Data Requirements: Guidance for Calculating Percent Survival in Seedling Emergence Studies
37. Christophe HL, Albert N, Martin Y, Mbaiguinam M (2019) Effect of organic fertilizers rate on plant survival and mineral properties of Moringa oleifera under greenhouse conditions. International Journal of Recycling of Organic Waste in Agriculture 8:123–130. https://doi.org/10.1007/s40093-019-0282-6
38. Sluiter A, Ruiz R, Scarlata C, et al (2008) Determination of Extractives in Biomass: Laboratory Analytical Procedure (LAP); Issue Date 7/17/2005

39. Sluiter A, Hames B, Hyman D, et al (2008) Determination of Total Solids in Biomass and Total Dissolved Solids in Liquid Process Samples Laboratory Analytical Procedure (LAP) Issue Date: 3/31/2008
40. Sacko O, Whiteman R, Kharel G, et al (2020) Sustainable Chemistry: Solubilization of Phosphorus from Insoluble Phosphate Material Hydroxyapatite with Ozonized Biochar. ACS Sustain Chem Eng 8:7068–7077. https://doi.org/10.1021/acssuschemeng.0c00601
41. Smith CR, Hatcher PG, Kumar S, Lee JW (2016) Investigation into the Sources of Biochar Water-Soluble Organic Compounds and Their Potential Toxicity on Aquatic Microorganisms. ACS Sustain Chem Eng 4:2550–2558. https://doi.org/10.1021/acssuschemeng.5b01687
42. Hirayama K, Maglinao R, Barbera E, Kumar S (2024) Production of phenolic monomers from lignin in hydrothermal medium: Effect of rapid heating and short residence time. Journal of Supercritical Fluids 205:. https://doi.org/10.1016/j.supflu.2023.106123
43. Liliana Krotz A, Giazzi G Sulfur determination in food by the Thermo Scientific FlashSmart Elemental Analyzer coupled with FPD Detector
44. Wang S-Q, Liu J-B, Kang J-Y, et al (2021) Root growth and morphology of switchgrass (Panicum virgatum L.) and bushclover (Lespedeza davurica S.) in mixed plantation under varying soil water and phosphorus supply conditions. Pak J Bot 53:. https://doi.org/10.30848/PJB2021-4(41)
45. Maryland Department of Natural Resources (2020) Native Plant Profile: Switchgrass (Panicum virgatum)
46. Gorlitsky LE, Sadeghpour A, Hashemi M, et al (2015) Biomass vs. quality tradeoffs for switchgrass in response to fall harvesting period. Ind Crops Prod 63:311–315. https://doi.org/10.1016/j.indcrop.2014.10.012
47. Brown C, Griggs T, Keene T, et al (2016) Switchgrass Biofuel Production on Reclaimed Surface Mines: I. Soil Quality and Dry Matter Yield. Bioenergy Res 9:31–39. https://doi.org/10.1007/s12155-015-9658-2
48. Galluzzi G, Plaza C, Priori S, et al (2024) Soil organic matter dynamics and stability: Climate vs. time. Science of the Total Environment 929:. https://doi.org/10.1016/j.scitotenv.2024.172441
49. Roper WR, Robarge WP, Osmond DL, Heitman JL (2019) Comparing Four Methods of Measuring Soil Organic Matter in North Carolina Soils. Soil Science Society of America Journal 83:466–474. https://doi.org/10.2136/sssaj2018.03.0105
50. Garten CT, Brice DJ, Castro HF, et al (2011) Response of “Alamo” switchgrass tissue chemistry and biomass to nitrogen fertilization in West Tennessee, USA. Agric Ecosyst Environ 140:289–297. https://doi.org/10.1016/j.agee.2010.12.016
51. Hou X, Amais RS, Jones BT, Donati GL (2016) Inductively Coupled Plasma Optical Emission Spectrometry. In: Encyclopedia of Analytical Chemistry. Wiley, pp 1–25
52. Vogel KP, Medill R, Masterson SD, et al (2017) Mineral element analyses of switchgrass biomass: Comparison of the accuracy and precision of laboratories. Agron J 109:735–738. https://doi.org/10.2134/agronj2016.08.0475

53. Zhang L, MacQueen A, Bonnette J, et al (2021) QTL × environment interactions underlie ionome divergence in switchgrass. G3: Genes, Genomes, Genetics 11:. https://doi.org/10.1093/g3journal/jkab144
54. Borne KE, Fassman-Beck EA, Winston RJ, et al (2015) Implementation and Maintenance of Floating Treatment Wetlands for Urban Stormwater Management. Journal of Environmental Engineering 141:. https://doi.org/10.1061/(asce)ee.1943-7870.0000959
55. Hall J, Muscarella R, Quebbeman A, et al (2020) Hurricane-Induced Rainfall is a Stronger Predictor of Tropical Forest Damage in Puerto Rico Than Maximum Wind Speeds. Sci Rep 10:. https://doi.org/10.1038/s41598-020-61164-2
56. Cui X, Hao H, He Z, et al (2016) Pyrolysis of wetland biomass waste: Potential for carbon sequestration and water remediation. J Environ Manage 173:95–104. https://doi.org/10.1016/j.jenvman.2016.02.049
57. White JE, Catallo WJ, Legendre BL (2011) Biomass pyrolysis kinetics: A comparative critical review with relevant agricultural residue case studies. J. Anal. Appl. Pyrolysis 91:1–33
58. Suresh Babu KKB, Nataraj M, Tayappa M, et al (2024) Production of biochar from waste biomass using slow pyrolysis: Studies of the effect of pyrolysis temperature and holding time on biochar yield and properties. Mater Sci Energy Technol 7:318–334. https://doi.org/10.1016/j.mset.2024.05.002
59. Giudicianni P, Cardone G, Ragucci R (2013) Cellulose, hemicellulose and lignin slow steam pyrolysis: Thermal decomposition of biomass components mixtures. J Anal Appl Pyrolysis 100:213–222. https://doi.org/10.1016/j.jaap.2012.12.026
60. Ghani WAWAK, Mohd A, da Silva G, et al (2013) Biochar production from waste rubber-wood-sawdust and its potential use in C sequestration: Chemical and physical characterization. Ind Crops Prod 44:18–24. https://doi.org/10.1016/j.indcrop.2012.10.017
61. Akhtar J, Saidina Amin N (2012) A review on operating parameters for optimum liquid oil yield in biomass pyrolysis. Renewable and Sustainable Energy Reviews 16:5101–5109
62. Loc NX, Phuong DTM (2025) Optimizing biochar production: a review of recent progress in lignocellulosic biomass pyrolysis. Front Agric Sci Eng 12:148–172. https://doi.org/10.15302/J-FASE-2024597
63. Khongphakdi P, Palamanit A, Phusunti N, et al (2020) Evaluation of Oil Palm Biomass Potential for Bio-oil Production via Pyrolysis Processes. International Journal of Integrated Engineering 12:. https://doi.org/10.30880/ijie.2020.12.02.027
64. Ashworth AJ, Sadaka SS, Allen FL, et al Influence of Pyrolysis Temperature and Production Conditions on Switchgrass Biochar for Use as a Soil Amendment
65. Muhammad N, Dai Z, Wang H, et al (2013) Impact of Pyrolysis Time and Temperature on Physicochemical Characteristics of Biochars from Wetland Plants. In: Functions of Natural Organic Matter in Changing Environment. Springer Netherlands, Dordrecht, pp 1039–1044
66. Djurdjevic M, Papuga S, Kolundzija A (2024) Analysis of the thermal behavior of a fixed bed reactor during the pyrolysis process. Hem Ind 78:29–40. https://doi.org/10.2298/HEMIND221217024D

67. Bieniek A, Jerzak W, Magdziarz A (2021) Experimental studies of intermediate pyrolysis of woody and agricultural biomass in a fixed bed reactor. E3S Web of Conferences 323:00003. https://doi.org/10.1051/e3sconf/202132300003
68. Batista RR, Gomes MM (2021) Effects of Chemical Composition and Pyrolysis Process Variables on Biochar Yields: Correlation and Principal Component Analysis. Floresta e Ambiente 28:. https://doi.org/10.1590/2179-8087-floram-2021-0007
69. Lynch J, Fox LJ, Owen Jr. JS, Sample DJ (2015) Evaluation of commercial floating treatment wetland technologies for nutrient remediation of stormwater. Ecol Eng 75:61–69. https://doi.org/10.1016/j.ecoleng.2014.11.001

Figures

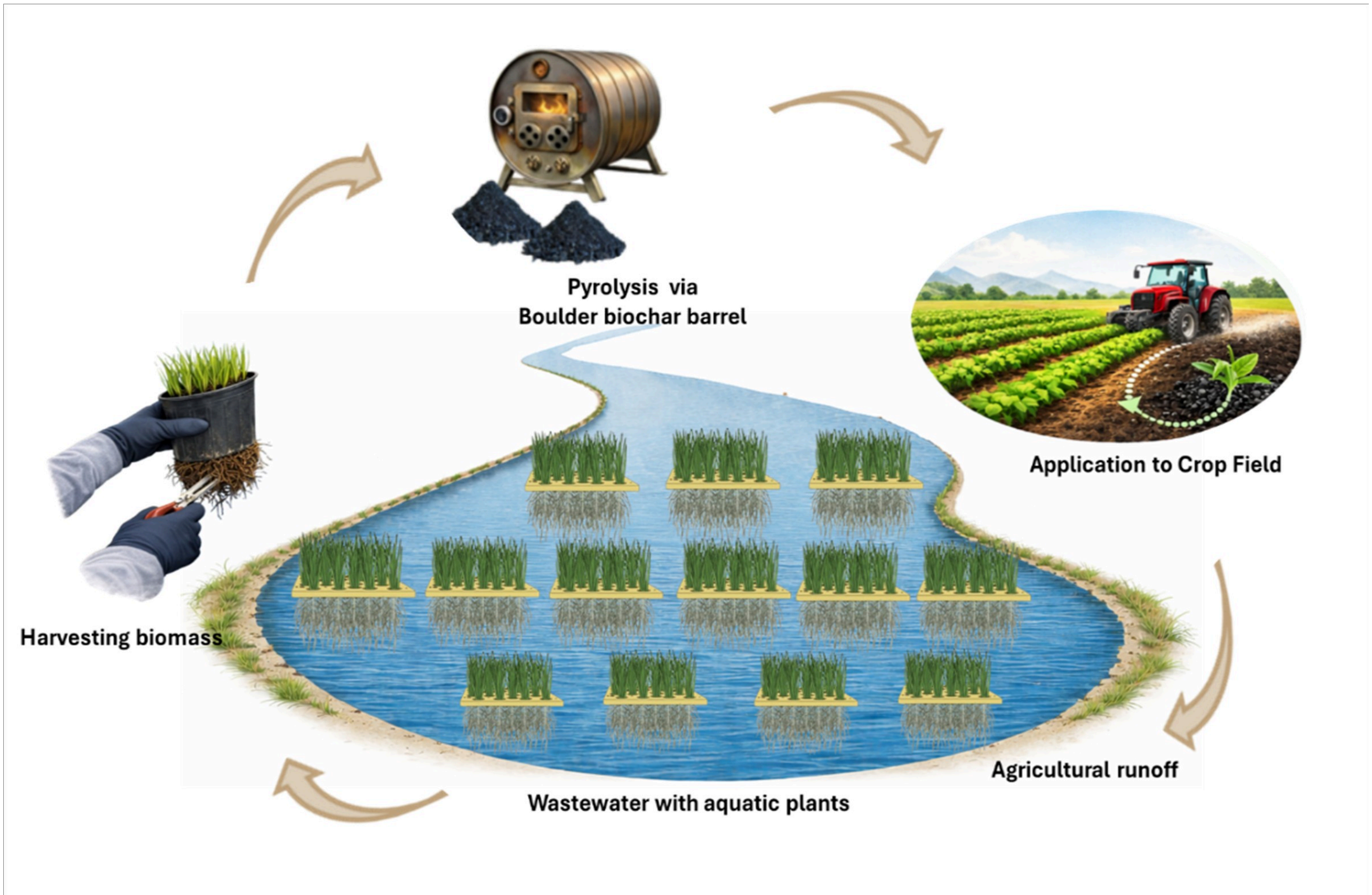

Figure 1

Conceptual illustration of a circular economy in a watershed system based on aquatic plant cultivation and bio-char application. Aquatic plants were grown in nutrient-rich wastewater to absorb nutrients and assist in phytoremediation. The harvested biomass was converted into biochar through pyrolysis in a bio-char reactor. The resulting biochar was then used in agricultural fields to enhance soil health and crop yields. Agricultural runoff returns to the watershed, where nutrients are once again absorbed by aquatic plants, closing the resource loop and supporting sustainable nutrient recycling and carbon sequestration.

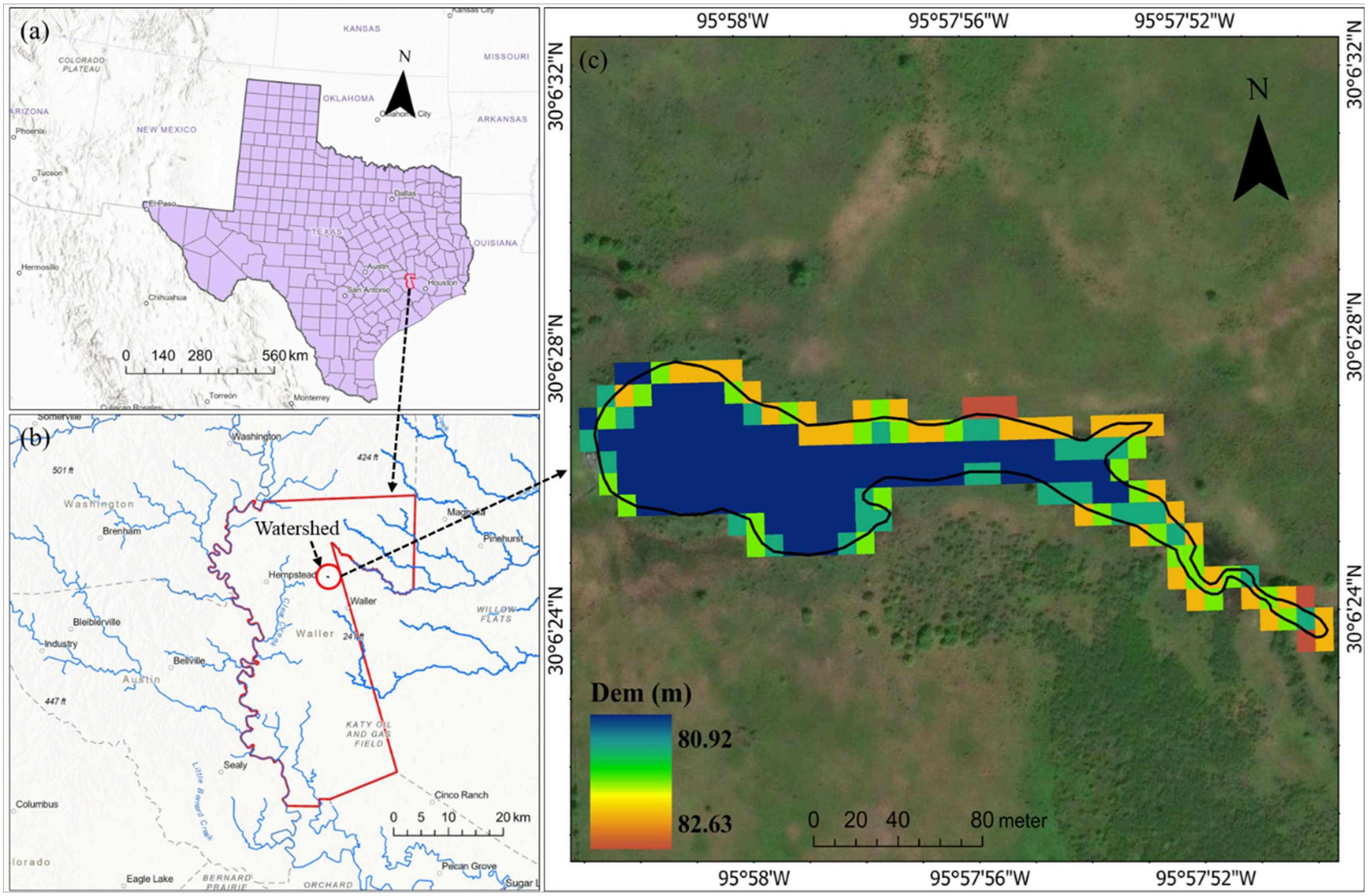

Figure 2

Geographic location and elevation profile of the PVAMU watershed, Waller County, Texas. The left panel (a-b) provides regional context, showing the watershed's location (red circle) within Waller County, Texas, relative to local drainage networks, streams, and nearby municipalities such as Hempstead and Waller. The right panel (c) shows a high-resolution Digital Elevation Model (DEM) overlaid on a satellite image, with a color gradient from blue to red indicating the watershed's local topography and delineated boundary.

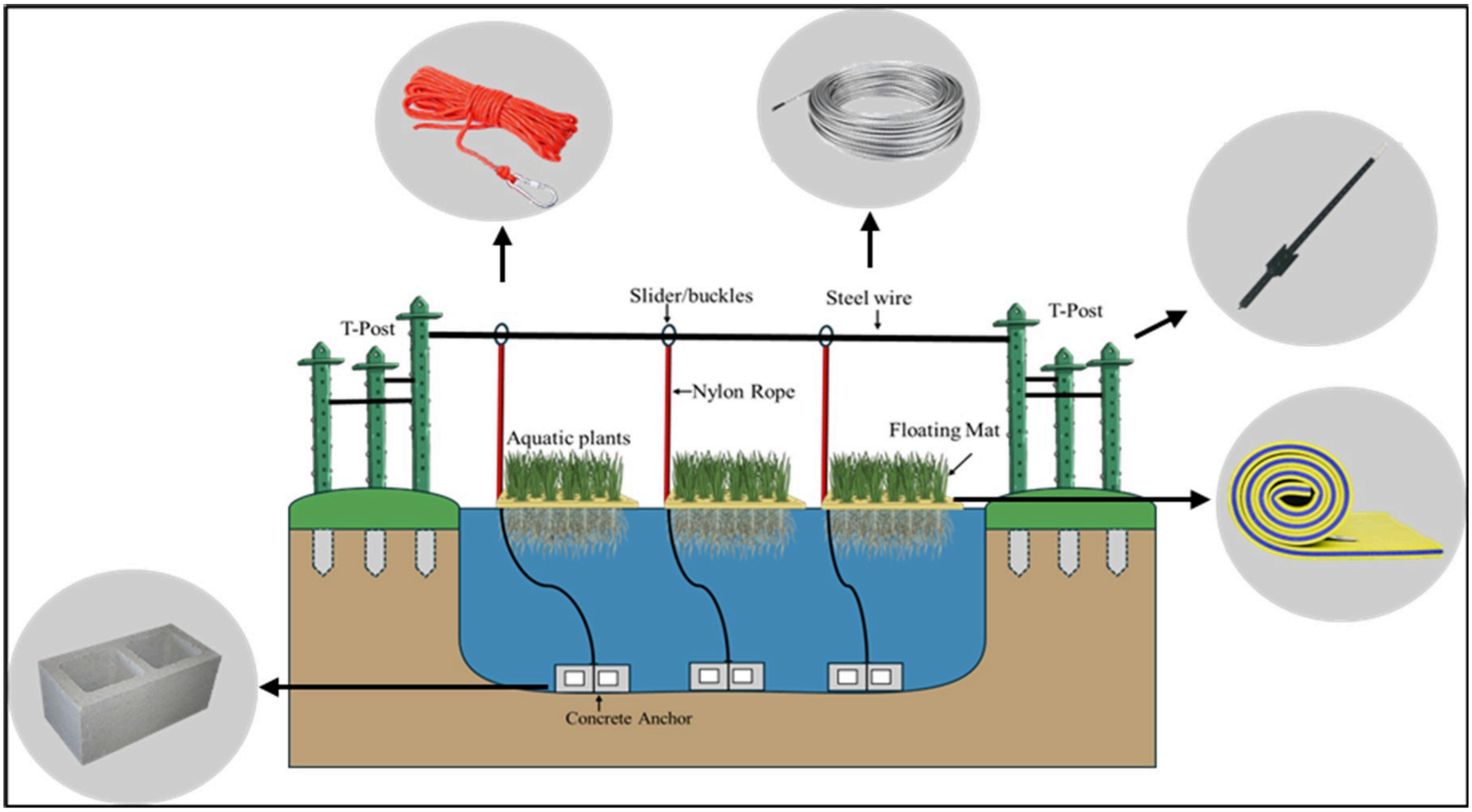

Figure 3

Schematic illustration of the experimental wetland mesocosm system used for evaluating plant-based remediation performance. The diagram shows a lined basin filled with water, with floating vegetative platforms positioned between reinforced side walls. Each floating unit consists of emergent macrophytes established on buoyant mats, with roots extending downward into the water column to facilitate nutrient uptake, contaminant removal, and microbial interactions within the rhizosphere. The platforms are secured in place using submerged concrete anchors connected by tethering lines to prevent lateral movement and maintain consistent spacing. Vertical red markers indicate sampling or monitoring points for water-quality measurements (e.g., nutrient concentrations, dissolved oxygen, pH, or contaminant levels) within each treatment zone. The system is designed to simulate controlled phytoremediation conditions and to compare treatment performance among replicated floating plant units under identical hydraulic and environmental settings.

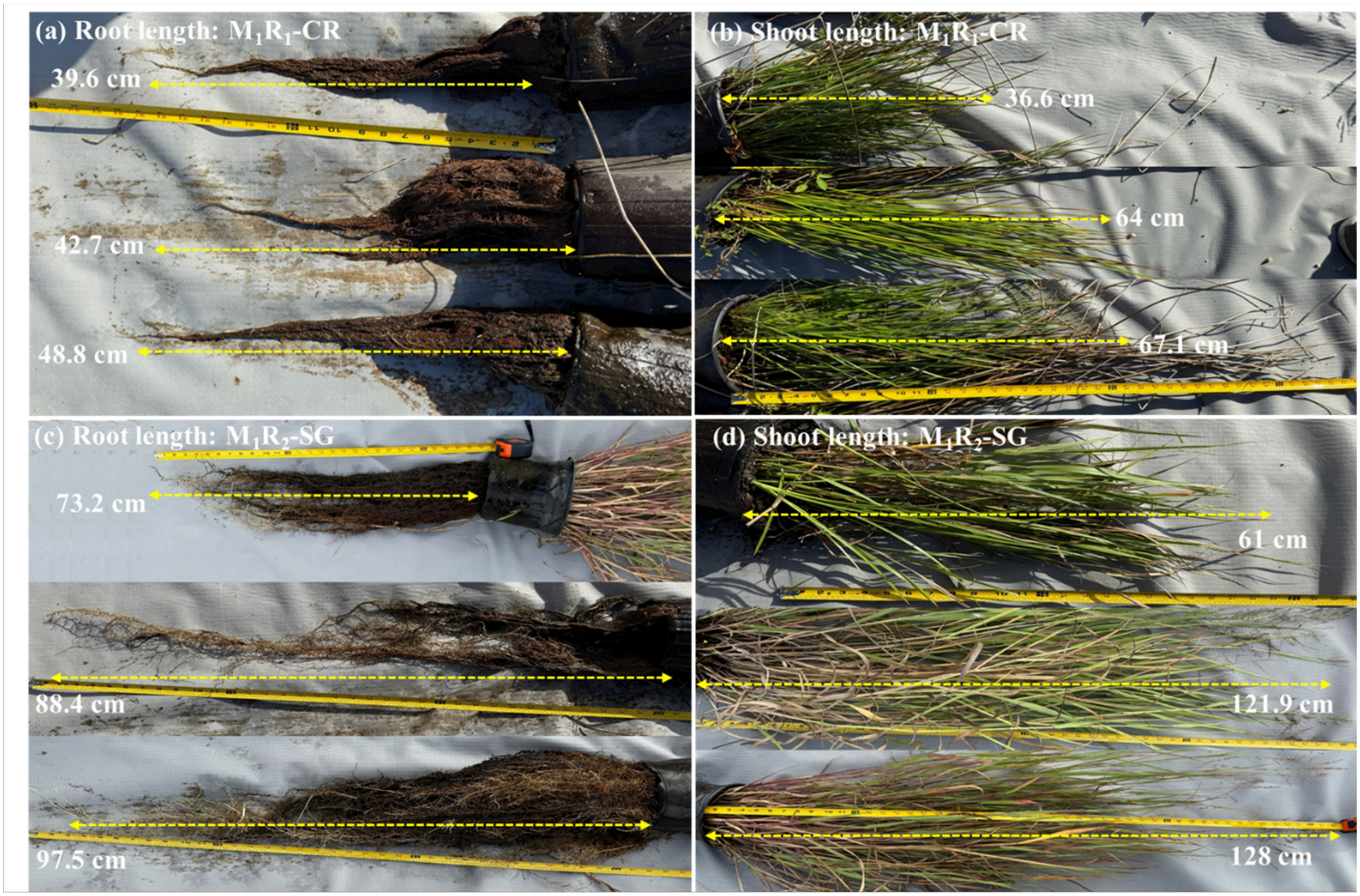

Figure 4

Comparative root and stem length measurements of common rush (CR) and switchgrass (SG) grow under field conditions of floating mat first and row first (M_1R_1). Here, (a) Root length and (b) stem length of common rush, showing root lengths of 39.6, 42.7, and 48.8 cm and stem lengths of 36.6, 64, and 67.1 cm. (c) Root length and (d) stem length of switchgrass, with root lengths of 73.2, 88.4 and 97.5 cm and stem lengths of 61, 121.9, and 128 cm. Measurements were recorded with a measuring tape, and dashed yellow lines indicate distances from the crown to the root tip or the stem apex. Switchgrass exhibited substantially greater root and stem elongation than common rush under identical conditions.

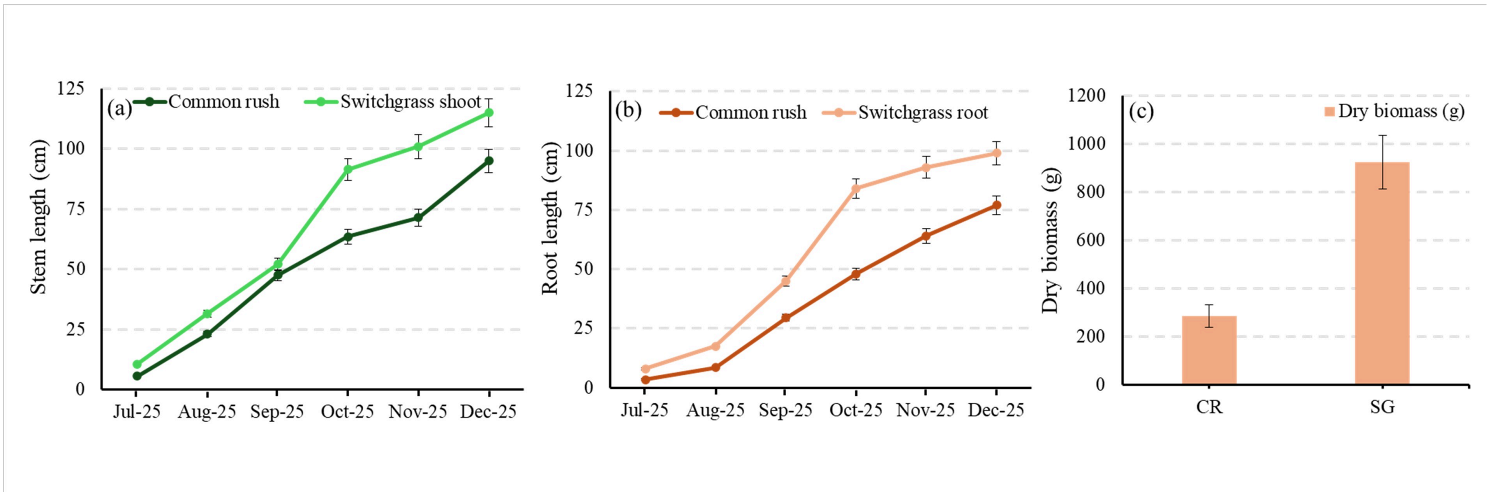

Figure 5

Cultivation of common rush and Switchgrass. Here, the longitudinal monitoring of their stem and root growth in FTWs is shown (a-b). Switchgrass exhibited greater stem and root development than common rush. The dry biomass of common rush and switchgrass by the end of the harvesting period in December 2025. CR: common rush; SG: Switchgrass (c).

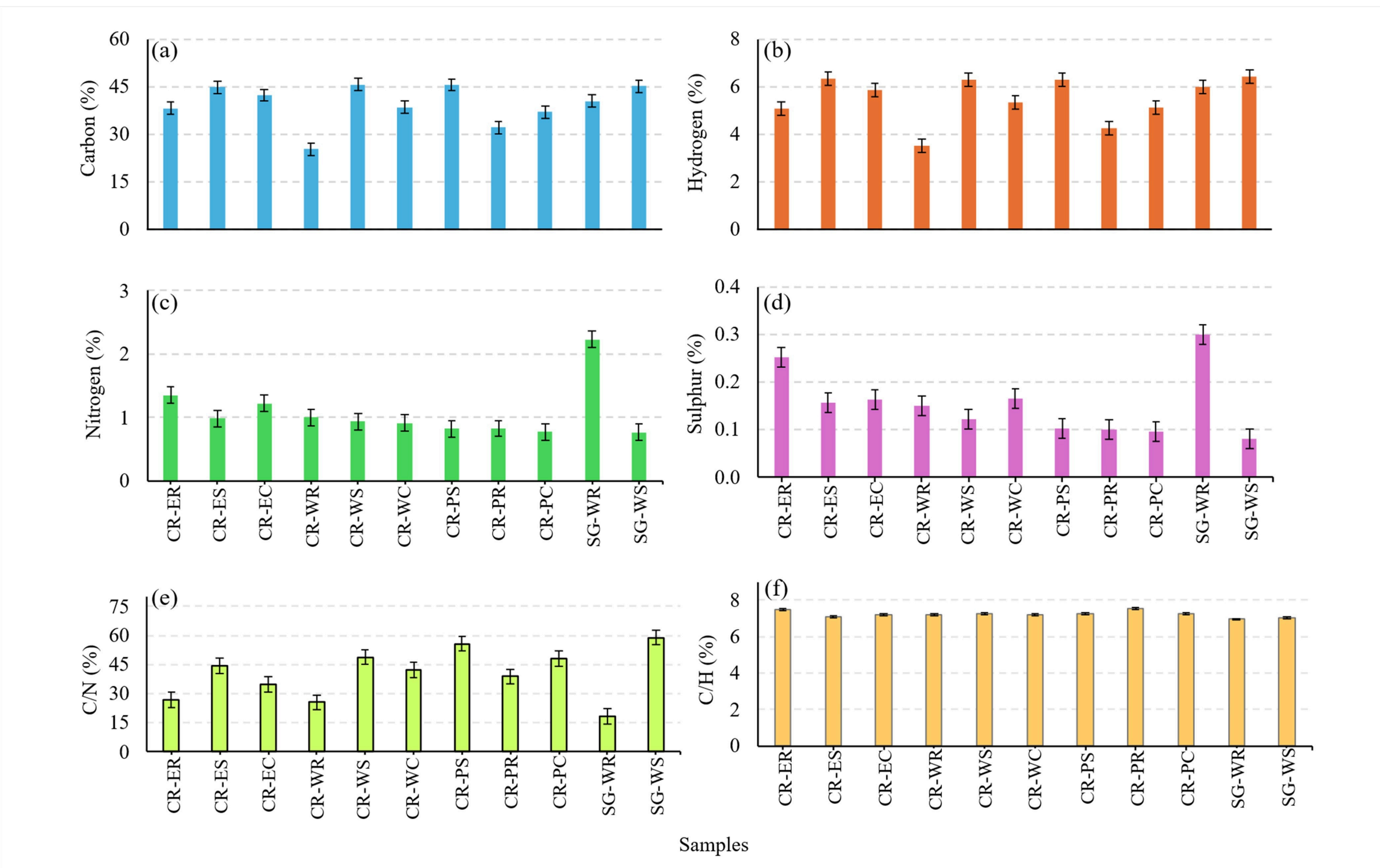

Figure 6

Elemental analysis of different biomass. Here, the concentrations of (a) carbon (C), (b) hydrogen (H), (c) nitrogen (N), and (d) sulfur (S), along with the ratios (e) C/N (%) and (f) C/H (%) in aquatic plant biomass are shown. The abbreviations are: CR-ER: common rush-edge root; CR-ES: common rush-edge stem; CR-EC: common rush-edge combined; CR-WR: common rush-watershed root; CR-WS: common rush-watershed stem; CR-WC: common rush-watershed combined; CR-PS: common rush-pool stem; CR-PR: common rush-pool root; CR-SPC: common rush-pool combined; SG-WR: switchgrass-watershed root; SG-WS: switchgrass-watershed stem.

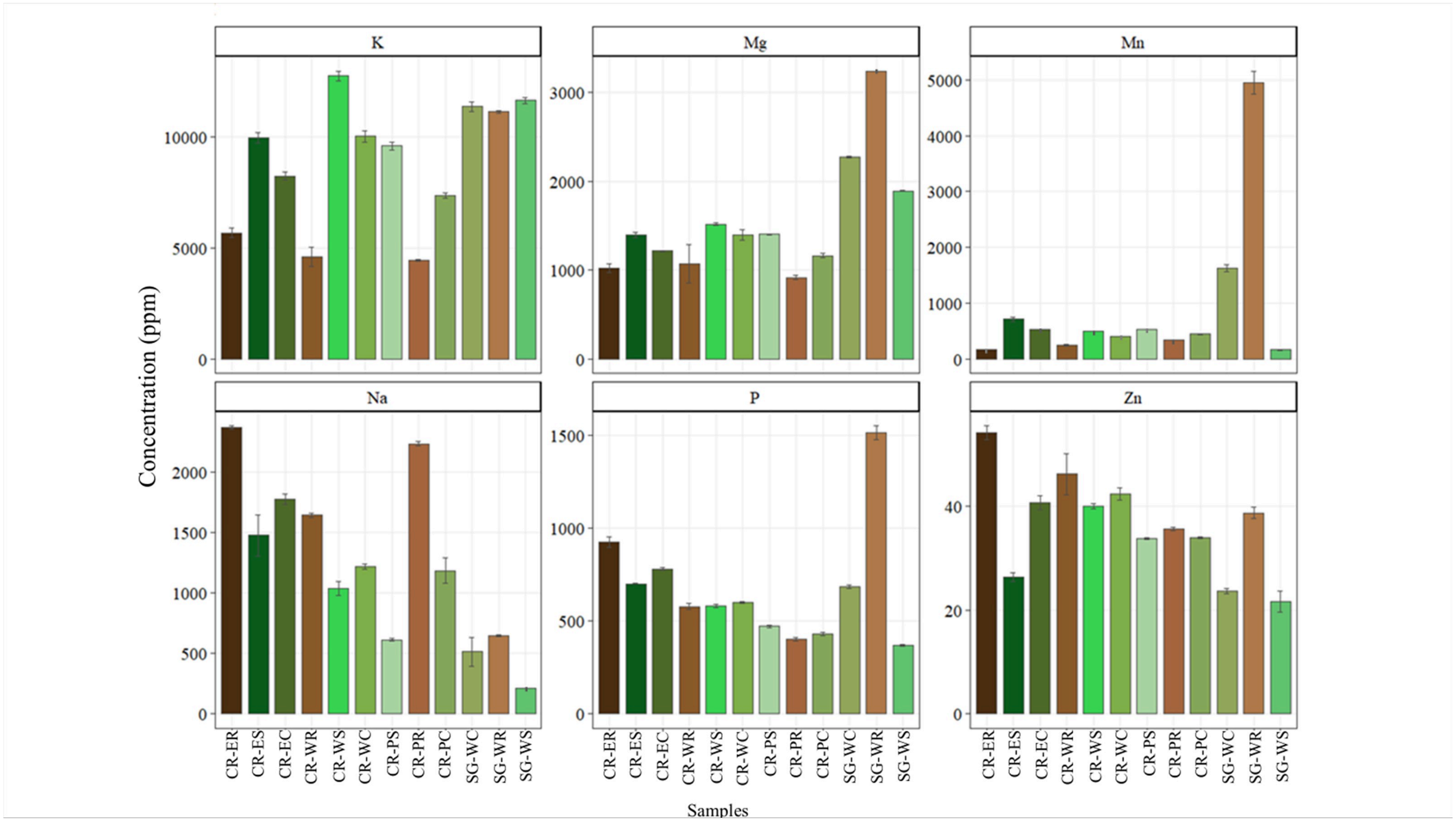

Figure 7

Element concentrations (K, Mg, Mn, Na, P, and Zn) at the edge, watershed, pool, and switchgrass systems varied significantly. Abbreviations: CR-ER: common rush-edge root; CR-ES: common rush-edge stem; CR-EC: common rush-edge combined; CR-WR: common rush-watershed root; CR-WS: common rush-watershed stem; CR-WC: common rush-watershed combined; CR-PS: common rush-pool stem; CR-PR: common rush-pool root; CR-SPC: common rush-pool combined; SG-WR: switchgrass-watershed root; SG-WS: switchgrass-watershed stem; SG-WC: switchgrass-watershed combined

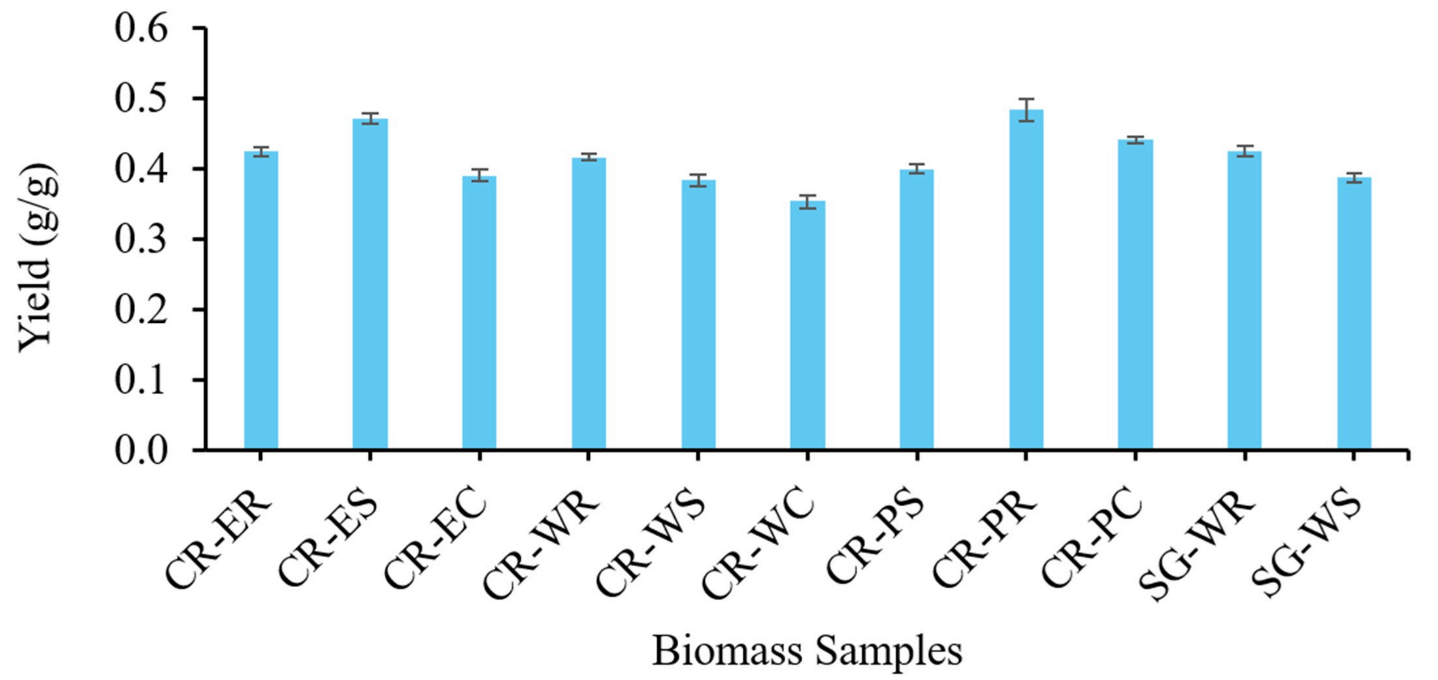

Figure 8

Common rush and switchgrass yield based on a feed varied from 15-30 g. Abbreviations: CR-ER: common rush-edge root; CR-ES: common rush-edge stem; CR-EC: common rush-edge combined; CR-WR: common rush-watershed root; CR-WS: common rush-watershed stem; CR-WC: common rush-watershed combined; CR-PS: common rush-pool stem; CR-SPR: common rush-pool root; CR-PC: common rush-pool combined; SG-WR: switchgrass-watershed root; SG-WS: switchgrass-watershed stem.

Supplementary Files

This is a list of supplementary files associated with this preprint. Click to download.

- SupplementaryInformation.docx